2017

New Methods to Estimate Abundance from Unmarked Populations Using Remote Camera Trap Data

Anna K. Moeller
University of Montana

NEW METHODS TO ESTIMATE ABUNDANCE FROM UNMARKED POPULATIONS USING REMOTE CAMERA TRAP DATA

By

ANNA KATHERINE MOELLER

B.S., University of Puget Sound, Tacoma, Washington, 2012

Thesis

presented in partial fulfillment of the requirements
for the degree of

Master of Science
in Wildlife Biology

The University of Montana
Missoula, MT

May 2017

Approved by:

Scott Whittenburg, Dean of The Graduate School
Graduate School

Dr. Paul M. Lukacs, Chair
Wildlife Biology Program, Department of Ecosystem and Conservation Sciences

Dr. Michael Mitchell
Wildlife Biology Program, Montana Cooperative Wildlife Research Unit

Dr. Mark Hebblewhite
Wildlife Biology Program, Department of Ecosystem and Conservation Sciences

Dr. Jon Horne
Idaho Department of Fish and Game

Moeller, Anna K., M.S., May 2017 Wildlife Biology

New Methods to Estimate Abundance from Unmarked Populations Using Remote Camera Trap Data

Chairperson: Dr. Paul M. Lukacs

ABSTRACT

Abundance estimates are central to the field of ecology and are an important tool for wildlife managers. While many tools are available for estimating abundance from individually identifiable animals, it is much more difficult to estimate abundance of unmarked animals. Most species have no natural markings and capturing them to apply artificial marks is invasive. One step toward noninvasive abundance estimation is the use of passive "traps" such as remote cameras or acoustic recording devices. The continuous-time data from these traps can be used to estimate abundance, although most available methods still require individually identifiable animals. There is a great need for methods to estimate abundance from unmarked populations using these trap data. We developed three methods for estimating abundance of unmarked animals from remote camera trap data. We worked outside the conventional capture-recapture framework to rethink how continuous remote data are handled. In Chapter 1, we developed an Instantaneous Sampling (IS) estimator based in sampling theory that treats remote camera data like point counts. In Chapter 2, we applied a time-to-event framework to develop a Space-to-Event (STE) and Time-to-Event (TTE) model to estimate abundance from trapping rate. We validated these methods on simulated populations with known abundance. All three methods produced unbiased estimates of abundance, regardless of animal movement rate. We performed a case study in which we estimated elk abundance from remote camera trap data in two study areas in Idaho. Estimates in one study area were comparable to an independent estimate of abundance from aerial surveys. In the other study area, other abundance methods are hard to implement, so our three models produced the first elk abundance estimates. The three methods developed here represent new ways of thinking about continuous-time remote camera data. These new methods allow biologists to estimate abundance from unmarked populations without tracking individuals over time. They have wide applications across species; biologists can select the method that best meets their specific circumstances. All three methods greatly reduce the amount of data required for analysis, which makes them practical management tools.

TABLE OF CONTENTS

Abstract ii

Acknowledgments iv

A note on authorship v

List of Figures vi

Chapter 1: An instantaneous sampling method for estimating abundance of unmarked animals .. 1

Abstract 1

Introduction 1

Methods 4

Instantaneous Sampling Estimator 4

Variance 5

Simulation Study 5

Estimating Elk Abundance in Idaho 6

Results 8

Simulation 8

Field Test 8

Discussion 9

Literature Cited 11

Figures 14

Chapter 2: Two new models to estimate abundance using time-to-event analysis 17

Abstract 17

Introduction 18

Methods 21

Space-to-Event Model 21

Time-to-Event Model 24

Simulation 26

Estimating elk abundance 27

Results 29

Simulation 29

Field 30

Discussion 30

Literature Cited 34

Figures 38

ACKNOWLEDGMENTS

Funding and support for this project was provided by Idaho Department of Fish and Game (IDFG), the University of Montana, the W.A. Franke College of Forestry and Conservation, and the Montana Cooperative Research Unit. IDFG provided data, equipment, and numerous hours of field labor to make this project possible.

First and foremost, I'd like to thank my advisor, Dr. Paul Lukacs. I am truly honored to work with you and call you a mentor and a friend. I can't imagine having a more supportive, patient advisor to guide me through the ups and downs of research. I know I've only tapped the depth of your knowledge and I look forward to learning from you throughout my career.

I owe deep thanks to my other committee members. Dr. Mike Mitchell, thank you for explaining to me what research is. Your insightful questions and guidance have helped me grow as a scientist and a professional. Thank you, Dr. Mark Hebblewhite, for your boundless enthusiasm, creativity, and scientific insight. Thank you to Dr. Jon Horne for helping to make our daunting field season possible.

The field work for this project was due to a huge collaboration of people. I am especially grateful to Molly McDevitt, who consistently pulled off super-human tasks with a grin on her face. Special thanks are due to Kaitlyn Reintsma, Gus Geldersma, and Liam Rossier, who undertook tough conditions with professionalism and positivity. Thank you to Katie Groth, Nikie Bilodeau, Joel Sauder, Alan Harrington, Sierra Robatcek, Brittany Deranleau, and the many other technicians and volunteers. Thank you to Chris Gaughan, Barb Moore, Laura Wolf, and the other IDFG biologists who provided equipment, knowledge, and field assistance. Molly, Carly Folsom, and Chuck Taylor managed to classify 1.3 million pictures in a matter of months – a feat I know few others could pull off. This project was a collaboration with the US Forest Service,

Bureau of Land Management, the State of Idaho, Potlatch Corporation, Molpus Timberlands Management, Hancock Forest Management, and private landowners, who granted access to our field sites.

Tina Anderson fielded dozens of travel forms and managed to keep everything straight when I got lost in a sea of paperwork. Jeanne Franz and Robin Hamilton helped keep me on target with my requirements. I am deeply grateful to Dr. Gretchen McCaffery for keeping me sane while writing up this huge project. Thank you to Dr. Mark Hurley for facilitating this project from the beginning.

Finally, thank you to my colleagues and friends who have guided me through graduate school. To all my fellow Lukacs incubees – Jenny Helm, Charlie Henderson, Dr. Rebecca McCaffery, Dr. Josh Nowak, Kelsey Wellington and Dr. Sara Williams – your knowledge, friendship, and advice have been my lifeline. To all my friends in the Wildlife Biology program, thank you for your conversations, insight, and support. Thanks always to my family, who have my back, no questions asked.

A NOTE ON AUTHORSHIP

Throughout this thesis I use the term "we" in order to recognize the collaborators who contributed valuable input, edits, and field assistance to this project.

LIST OF FIGURES

Chapter 1

Figure 1-1. Sampling scheme for estimating elk abundance with the Instantaneous Sampling method in the Beaverhead and Panhandle study areas (gray areas, inset map; Beaverhead shown in detail, main map). In each study area, we delineated elk winter range (black grid cells) and randomly selected nine 1.5x1.5 km grid cells (red). We divided each selected grid cell into nine 500x500m sub-cells and placed one camera in each, in a nested design. We deployed cameras from February 1 – 29, 2016 in both study areas. 14

Figure 1-2. Histogram of abundance estimates from 1,000 simulated populations using the Instantaneous Sampling estimator. Animals in simulated populations took fixed steps with length 1 (a) or length 3 (b). The red line is truth (N = 15) and the blue line is mean estimated abundance. 15

Figure 1-3. Instantaneous Sampling estimates of elk abundance (circles) for the Beaverhead and Panhandle study areas with 95% confidence intervals and the 2008 – 09 aerial survey estimate for the Beaverhead (cross). The IS method estimated 1,613 elk (SE 530) in the Beaverhead and 1,258 elk (SE 596) in the Panhandle for February 2016..... 16

Chapter 2

Figure 2-1. Conceptual diagram of the Space-to-Event (STE) model. An array of grid cells with known area are randomly sampled. In the case of cameras, the shape of the grid cell is a circular sector rather than a rectangle. On each occasion $j = 1, 2, \ldots, J$ the observed space-to-event S_j is the number of the first trap $i = 1, 2, \ldots, M$ (here, $M = 3$) that contains the species of interest. a) At

j = 1, the first trap that contains an animal is trap 3, so S_1 = 3. b) At j = 2, although both traps 2 and 3 contain an animal, we record the first trap in the series {2, 3}, so S_2 = 2..... 38

Figure 2-2. Conceptual diagram of the Time-to-Event (TTE) model at a single trap i and a single occasion j. When using cameras, the shape of the grid cell is a circular sector rather than a rectangle. Successive samples are taken at each period k = 1, 2, …, K (Here, K = 3). The observed time-to-event T_{ij} is equal to the period k in which the grid cell first contains an animal. There are no animals in the trap in a) k = 1 or b) k = 2, so for this camera and sampling occasion, T_{ij} = 3..... 39

Figure 2-3. Histogram of abundance estimates from 10,000 simulated populations using the Space-to-event (a, b) and Time-to-Event (c, d) models. Simulated animals took fixed steps with either length 1 (a, c) or length 3 (b, d). The red line is truth (N = 15) and the blue line is mean estimated abundance. 40

Figure 2-4. Elk group size from the Beaverhead and Panhandle camera data in February 2016. Most elk occurred in groups of 1 or 2..... 41

Figure 2-5. Space-to-Event (STE) and Time-to-Event (TTE) estimates of elk abundance in the Beaverhead and Panhandle study areas with 95% confidence intervals. In the Beaverhead study area, the STE model estimated 1,405 elk (SE 133.4) and the TTE model estimated 2,217 elk (SE 211.6). In the Panhandle study area, the STE model estimated 1,368 elk (SE 238.4) and the TTE estimated 5,670 elk (SE 633.4). 42

CHAPTER 1: AN INSTANTANEOUS SAMPLING METHOD FOR ESTIMATING ABUNDANCE OF UNMARKED ANIMALS

ABSTRACT

Abundance estimates are central to wildlife management but can be expensive, time-consuming, and dangerous to obtain. Remote camera traps are a way to estimate abundance non-invasively, but current methods are severely limited when animals are not uniquely identifiable. For species such as elk (*Cervus elaphus*), assumptions of closure are hard to meet and independent detections are difficult to define. To address these challenges, we developed an Instantaneous Sampling (IS) density estimator for cameras. This method treats remote camera data as a random sample of density, similar to fixed area sampling. We evaluated this estimator with a simulation study and applied it to camera data from two field settings to estimate elk abundance. Results from the simulation study suggest that the IS method is an unbiased estimator of abundance. This new method allowed us to estimate elk population size in two distinct habitats, including one where no elk abundance estimates had ever been performed due to dense vegetation and steep topography. This new method is a non-invasive way to estimate abundance of unmarked animals and has broad applicability across many species. It reframes the traditional approach to camera trap data by using random samples of density instead of monitoring individuals.

INTRODUCTION

Abundance estimates are fundamental to the field of ecology and are an important piece of information for wildlife managers (Andrewartha and Birch 1954). Wildlife biologists estimate abundance to monitor populations' responses to changes in habitat, climate, or other species. Abundance allows them to quantify the strength of inter-species interactions. Managers use

abundance to prioritize actions with the largest impact on a target species and then measure the success of those actions. For hunted species like deer (*Odocoileus* spp.) and elk (*Cervus elaphus*), abundance is important in setting harvest quotas and ensuring that harvest goals are met (Williams et al. 2002).

Deer and elk abundance is vital information to managers, but it can be dangerous and expensive to estimate. Aerial surveys are common for estimating abundance, but aviation accidents are all too common and pose a fatal risk to wildlife professionals (Sasse 2003). For example, of all known job-related deaths, two-thirds were due to aviation accidents (Sasse 2003). Beyond the risk to human safety, aerial surveys are extremely expensive, can be stressful to animals, and are difficult to implement in low snow winters. Furthermore, aerial surveys are only practical in some deer and elk habitats; dense vegetation shields animals from view and makes aerial surveys impossible (Samuel et al. 1987). Wildlife managers in forested areas must instead rely on less informative abundance indices or trend estimates. Safer, cheaper methods to estimate deer and elk abundance from the ground would help alleviate these challenges.

Remote cameras are a non-invasive and cost-effective way to estimate abundance for many species but present many challenges when applied to deer and elk (O'Connell et al. 2011). The majority of camera trap abundance studies use capture-recapture or mark-resight models that require individually identifiable animals (Foster and Harmsen 2012, Burton et al. 2015). These are useful for species with unique markings like tigers (*Panthera tigris*; Karanth 1995) but less so for animals without natural individual markings. Marking deer and elk is invasive and frequently requires extensive helicopter use. To decrease the number of costly helicopter surveys, biologists need an alternative method to estimate abundance from camera trap data for species with no individually identifiable characteristics.

Three methods currently exist to estimate abundance from unmarked animals from cameras, but these are limited when applied to deer and elk. These methods are the Spatial Count (SC) model (Chandler and Royle 2013), the Random Encounter Model (REM; Rowcliffe et al. 2008), and N-mixture models (Royle 2004). They require assumptions that can be difficult to meet, especially with large ungulates. First, N-mixture models and the SC model are highly sensitive to camera spacing (Keever 2014, Royle et al. 2014). Cameras must be placed with great attention to animal home ranges and movement patterns so that individuals are captured on exactly one camera or on multiple cameras at different distances from the home range center, respectively. Home ranges and movement can be very difficult to know ahead of time or calculate at all (Chandler and Royle 2013). Second, N-mixture models assume closure at the home range level (Royle 2004). While this may work for fish in a lake, it is likely to be violated by ungulates with large and uneven home ranges. Next, the REM requires an independent estimate of animal movement rates, which can be difficult to obtain (Rowcliffe et al. 2008). Finally, the REM requires that each detection of an animal at a camera is independent of previous detections. It is particularly challenging to define independent detections at cameras, so they are arbitrarily defined by various criteria like time cutoffs (e.g., 30 min, 60 min, 1 day; Burton et al. 2015).

Abundance estimation methods based in sampling theory may be able to overcome these challenges. Sampling theory allows ecologists to describe a population by the characteristics of a sample of that population (Cochran 1977). For example, the count of animals in a sampled area can be used to estimate abundance in a larger area of interest when the sampled area and study area size are known. This is the basis for many wildlife abundance estimation methods, including point counts, line transects, and distance sampling (Williams et al. 2002).

We used sampling theory to develop a novel Instantaneous Sampling (IS) method to estimate abundance from camera data. Due to the properties of probability, the IS estimator is not sensitive to camera spacing, does not assume small-scale closure, and does not require estimates of movement rates or arbitrary definitions of independent detections. We evaluated this estimator on simulated data and applied it to field data to estimate elk abundance in two study sites. In one study area, managers currently estimate elk abundance with aerial surveys but aim to decrease flight hours in the future. We compared abundance estimates from the IS method to the estimate from a recent aerial survey in this area. In the other study area, dense vegetation precludes aerial surveys; our application of the IS method produced the area's first elk abundance estimate.

METHODS

Instantaneous Sampling Estimator

We used sampling theory to develop an Instantaneous Sampling (IS) density estimator for cameras. This approach treats camera data as spatially and temporally replicated fixed-area counts. The number of animals in a given picture is a sample of density at an instant in time in the camera's viewable area. When cameras are deployed to points selected at random with known selection probability, each photo is an instantaneous snapshot of overall density in the study area. Because cameras collect data continuously, photos across time serve as temporal replicates. Over many spatial and temporal replicates, the mean count n_{ij} at location $i = 1, 2, \ldots, M$ and occasion $j = 1, 2, \ldots, J$ is an estimate of local density (D) in the camera's viewable area (a_{ij}), following:

$$\widehat{D} = \frac{1}{J} \cdot \frac{1}{M} \sum_{j=1}^{J} \sum_{i=1}^{M} \frac{n_{ij}}{a_{ij}} \qquad \text{(Equation 1)}$$

We calculate the camera's viewable area (a_{ij}) as a circular sector defined by the lens angle (θ_{ij}) in degrees and the maximum viewable distance (r_{ij}) as

$$a_{ij} = \pi r_{ij}^2 \frac{\theta_{ij}}{360} \quad \text{(Equation 2)}$$

The maximum viewable distance is defined by the trigger distance if using motion-sensor cameras or field landmarks if using time lapse cameras.

Abundance ($\hat{N}$) is then derived by multiplying density by the study area size (A)

$$\widehat{N} = A * \widehat{D} \quad \text{(Equation 3)}$$

to provide inference to the entire study area.

Variance

Because the cameras were not redeployed at each time step, we used bootstrapping to estimate the variance of $\hat{N}$ (Efron and Tibshirani 1993). This helped account for any correlation among samples at a single camera. We sampled the cameras with replacement and created an encounter history with all observations at those cameras. We estimated variance as the standard deviation of a large number of abundance estimates from these datasets (e.g., 10,000 repetitions). In this analysis, bootstrapping was extremely efficient and not time-limiting.

Simulation Study

We performed a mechanistic simulation to verify that the Instantaneous Sampling estimator returns an unbiased estimate of abundance and its variance. We simulated two populations of 15 animals moving at different speeds. Every "animal" was an independent uncorrelated random walk with fixed step lengths and random turning angles, bounded within a 30x30 unit area. All animals in the first population took steps of length 1 and animals in the second population took steps of length 3. Each random walk returned a list of xy-coordinates for 1,000 steps. We sampled every tenth step and determined whether the animal was within one of

10 randomly placed 1x1 unit square "cameras". At each camera and step, animals were "captured" if their random walk coordinates fell within the camera's coordinates, inclusive of two borders. We created a spatially and temporally replicated encounter history from the count of animals at each camera and time step. We applied the IS estimator to this encounter history to estimate abundance for the study area. We repeated this for 1,000 datasets and estimated variance with the standard deviation of these abundance estimates.

Estimating Elk Abundance in Idaho

We applied the Instantaneous Sampling method to camera trap data to estimate elk abundance in the Idaho Panhandle and Beaverhead Mountains (Figure 1-1). The Beaverhead study area is characterized by high-desert grass-sagebrush communities and windswept hills. Elk are mostly unrestrained by topography or dense vegetation. Aerial surveys that are corrected for sightability bias (Samuel et al. 1987, 1992) are used to estimate elk abundance every few years in this area, against which we compared estimates from the IS method. In contrast, the Panhandle study area is a mixed-conifer forest with a patchwork of active logging. Dense vegetation and steep slopes prevent biologists from performing aerial surveys, so no abundance estimates currently exist.

We deployed 160 remote cameras on elk winter range in February 2016. To define Beaverhead winter range, we created a 2km buffer around 3,525 Global Positioning System (GPS) locations from December 18, 2014 – March 20, 2015 from 33 calf and female elk. The 493 km^2 study area spanned an elevation range of 1,279 – 2,722 m. We defined the Panhandle study area as elk winter range as defined by Idaho Department of Fish and Game (IDFG).

We randomly selected nine plots in each study area using Generalized Random Tessellation Sampling (GRTS; Stevens and Olsen 2004) with the R package spsurvey (Kincaid

and Olsen 2011, R Core Team 2015). GRTS sampling allows the user to "replace" plots in the ordered sample, so we eliminated two plots that were adjacent to higher ranked plots (Stevens and Olsen 2004). We also replaced two plots due to lack of accessibility during winter and/or lack of landowner approval.

We divided each 1.5x1.5 km plot into nine equal sections and systematically placed one camera in each section. In two plots, we only deployed cameras in eight of the nine sub-plots due to access limitations. Within the bounds of the sub-plot, we targeted trails and ridges to maximize the probability of capture of elk, following general recommendations from camera trapping studies (O'Connell et al. 2011). We pointed cameras north to limit direct sunlight in the frame and cleared any vegetation obstructing the camera's view. The infrared-flash, motion-triggered cameras (Reconyx, Inc., Holmen, WI, USA) had high trigger sensitivity and took bursts of five pictures with no delay between trigger activations.

In the Panhandle study area, we placed 80 cameras (Reconyx model XR6) on trees at an approximate height of 8 – 10 feet. Because there were few or no trees in the Beaverhead study area, we placed 80 cameras (Reconyx models HC600, PC800, and PC900) on T-posts at an approximate height of 4 – 5 feet. In addition to the motion trigger, Beaverhead cameras took pictures every five minutes from 06:00 – 18:00. Beaverhead cameras had long, unimpeded views, so we placed flagging at known intervals and only counted elk within a set distance of the camera.

To obtain spatially and temporally replicated counts for the IS estimator, we counted all visible elk in a subset of photos taken between February 1 – 29, 2016. In the Beaverhead study area, we used photos taken on the hour, every hour, giving us 60 elk detections over the 80 cameras and 696 sampling occasions. In the Panhandle study area, we had fewer elk detections

so we extended the length of our sampling occasion. We sampled photos taken within the first 60 seconds of each hour and used the maximum count of elk in any single photo within that period. If no photos were taken during this time, we recorded a count of 0. We observed 21 elk detections over the 80 cameras and 696 sampling occasions.

We calculated the visible camera area in both study areas by camera specifications ("Trailcam Pro" 2017) using Equation 2. In the Beaverhead, we based visible camera area on the Reconyx HC600 model, letting $\theta = 42°$. We set $r = 50$m based on the flagging we deployed in the field. In the Panhandle, we let $\theta = 45.2°$ and $r = 18.3$m, the maximum trigger distance (Reconyx model XR6).

We estimated variance by bootstrapping the datasets 10,000 times for each study area and calculating the standard deviation of their abundance estimates.

RESULTS

Simulation

To evaluate abundance estimates from the IS estimator, we estimated abundance from simulated data with a known population size. We tested the estimator on two populations moving at different speeds to determine whether movement rate influenced abundance estimates. For the population of 15 with step length 1, the mean estimated abundance was 15.05 (SE = 4.29; Figure 1-2). For the population with step length 3, the mean estimated abundance was 15.14 (SE 4.18). These results demonstrated that the estimator performed well when individuals moved randomly among the cameras and that the estimator was not sensitive to movement rates of animals.

Field Test

To evaluate the Instantaneous Sampling estimator in a real-world setting, we applied it to data from two sets of camera data. In the Beaverhead study area, we estimated 1,613 elk (SE

530). The 95% confidence interval covered the 2008 – 09 aerial survey estimate of 2,272 elk in this area (Figure 1-3). In the Panhandle study area, we estimated 1,258 elk (SE 596), which was the first abundance estimate for this elk population. Based on harvest statistics and expert opinion, this estimate was within the range of expected values for the study area. Together, these results demonstrated that the IS estimator produced reasonable estimates when applied in a field setting.

DISCUSSION

The Instantaneous Sampling method developed here represents a shift in the way we think about camera data. Instead of identifying unique individuals for a capture-recapture framework, the IS method uses sample counts of the entire population. This allowed us to estimate elk abundance from camera data, which has never been done before. In the Beaverhead study area, the IS method produced a similar elk abundance estimate to previous aerial surveys. In the Panhandle study area, the IS method produced the very first elk abundance estimate because no other methods have been viable. These results are promising for future applications of this method in the field.

The IS method eliminates the major challenges associated with other abundance estimation methods for camera traps. Due to the properties of sampling theory, the IS method is not sensitive to camera spacing. Because each camera is a random sample of the population, cameras can be deployed without respect to individuals' home ranges and movement. Next, the IS estimator treats the viewable area in front of the camera as an entire plot rather than as a sample of some larger area. Therefore, there is no assumption of closure at the home range level. Next, the IS estimator does not require estimates of species movement rates or definition of independent detections by time cutoffs. Although some species neatly file past cameras, elk tend

to mill around them. Elk detections in this study lasted anywhere from one second to six hours; defining an independent detection by a single time cutoff was impractical. The IS estimator instead assumes that animals re-randomize between sampled photos at each camera, which is not necessarily violated by the same animal being present in two consecutive samples.

An additional benefit of this method is that it greatly reduces the number of photos needed for classification. Large-scale camera trapping studies produce enormous amounts of data. Classifying hundreds of thousands of photos is not sustainable as a long-term management tool. In this study alone, our cameras took 1.3 million photos in a 4-month field season. However, with this method we only had to analyze 4% of those pictures. The IS method is practical for managers who need real-time abundance estimates but have limited time and resources.

The assumptions of the IS method warrant further exploration in varied field settings. The estimator assumes that animals move randomly across the landscape with respect to the cameras. For some animals this is a relatively realistic approximation of movement, but this may not apply to all species. Future work may incorporate landscape covariates into the IS estimator to account for non-random movement. Next, the calculation of viewable area at the camera warrants further research. The viewable distance may change with weather, time of day, or photo quality. These same factors can also influence observer error in identifying species and counting individuals (Folsom 2017). Future applications may benefit by incorporating detection probability at the observer level.

For field implementation of this method, we suggest randomly deploying cameras that take pictures at predefined time intervals. Using only motion-sensor cameras introduces a level of uncertainty in the detection process. When motion-sensor cameras are used, occasions with no

photos can arise through two processes: either 1) animals were not present at the camera or 2) they were present and no picture was taken. Even though detection probability at the camera level can be quite high with certain models, we suggest eliminating this uncertainty. Many remote cameras can take both motion-triggered and time-lapse photos so this would not preclude collecting data for other uses.

The underlying theory of the IS method may be relevant to other remotely collected data like acoustic recording devices. The IS method also has broad applicability across many species with no natural identifying characteristics. This noninvasive method reframes the way we approach continuous, remotely-collected species data.

LITERATURE CITED

Andrewartha, H. G., and C. Birch. 1954. The distribution and abundance of animals. First edition. University of Chicago Press, Chicago.

Burton, A. C., E. Neilson, D. Moreira, A. Ladle, R. Steenweg, J. T. Fisher, E. Bayne, and S. Boutin. 2015. Wildlife camera trapping: a review and recommendations for linking surveys to ecological processes. Journal of Applied Ecology 52:675–685.

Chandler, R. B., and J. A. Royle. 2013. Spatially explicit models for inference about density in unmarked or partially marked populations. Annals of Applied Statistics 7:936–954.

Cochran, W. G. 1977. Sampling Techniques. Third edition. Wiley, New York.

Efron, B., and R. J. Tibshirani. 1993. An introduction to the bootstrap. Chapman & Hall, New York.

Folsom, C. 2017. Effect of photo quality on identification and count of populations in classifying camera trap photos. University of Montana.

Foster, R. J., and B. J. Harmsen. 2012. A critique of density estimation from camera-trap data.

Journal of Wildlife Management 76:224–236.

Karanth, K. U. 1995. Estimating tiger Panthera tigris populations from camera-trap data using capture-recapture models. Biological Conservation 71:333–338.

Keever, A. C. 2014. Use of N-mixture models for estimating white-tailed deer populations and impacts of predator removal and interspecific competition.

Kincaid, T. M., and A. R. Olsen. 2011. spsurvey: spatial survey design and analysis R package.

O'Connell, A. F., J. D. Nichols, and K. U. Karanth, editors. 2011. Camera traps in animal ecology: methods and analyses.

R Core Team. 2015. R: a language and environment for statistical computing. R Foundation for Statistical Computing, Vienna, Austria.

Rowcliffe, J. M., J. Field, S. T. Turvey, and C. Carbone. 2008. Estimating animal density using camera traps without the need for individual recognition. Journal of Applied Ecology 45:1228–1236.

Royle, J. A. 2004. N-Mixture Models for Estimating Population Size from Spatially Replicated Counts. Biometrics 60:108–115.

Royle, J. A., R. B. Chandler, R. Sollmann, and B. Gardner. 2014. Spatial capture-recapture. Elsevier.

Samuel, M. D., E. O. Garton, M. W. Schlegel, and R. G. Carson. 1987. Visibility bias during aerial surveys of elk in northcentral Idaho. Journal of Wildlife Management 51:622–630.

Samuel, M. D., R. K. Steinhorst, E. O. Garton, and J. W. Unsworth. 1992. Estimation of wildlife populations ratios incorporating survey design and visibility bias. Journal of Wildlife Management 56:718–725.

Sasse, D. B. 2003. Job-related mortality of wildlife workers in the United States, 1937-2000.

Wildlife Society Bulletin 31:1015–1020.

Stevens, D. L., and A. R. Olsen. 2004. Spatially balanced sampling of natural resources. Journal of the American Statistical Association 99:262–278.

TrailcamPro. 2017. Reconyx game camera reviews. https://www.trailcampro.com.

Williams, B. K., J. D. Nichols, and M. J. Conroy. 2002. Analysis and management of animal populations. Academic Press.

FIGURES

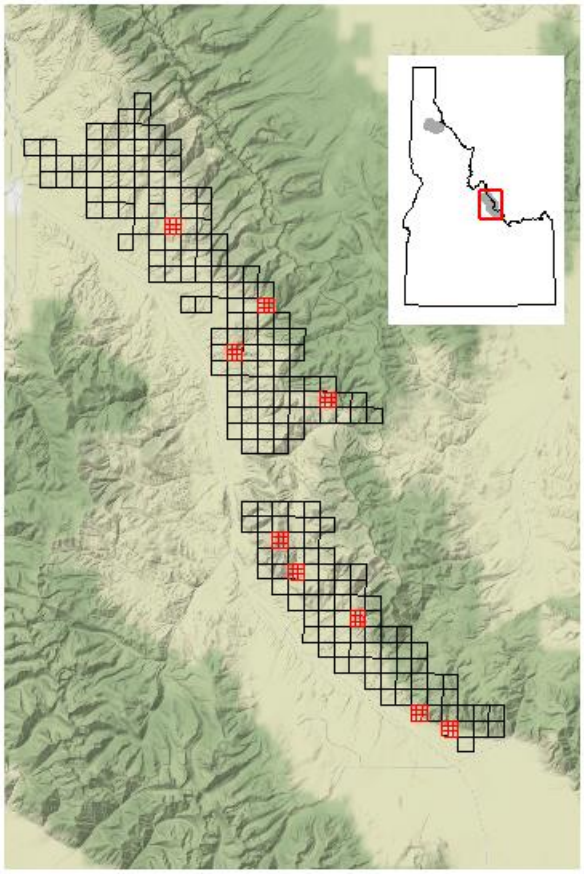

Figure 1-1. Sampling scheme for estimating elk abundance with the Instantaneous Sampling method in the Beaverhead and Panhandle study areas (gray areas, inset map; Beaverhead shown in detail, main map). In each study area, we delineated elk winter range (black grid cells) and randomly selected nine 1.5x1.5 km grid cells (red). We divided each selected grid cell into nine 500x500m sub-cells and placed one camera in each, in a nested design. We deployed cameras from February 1 – 29, 2016 in both study areas.

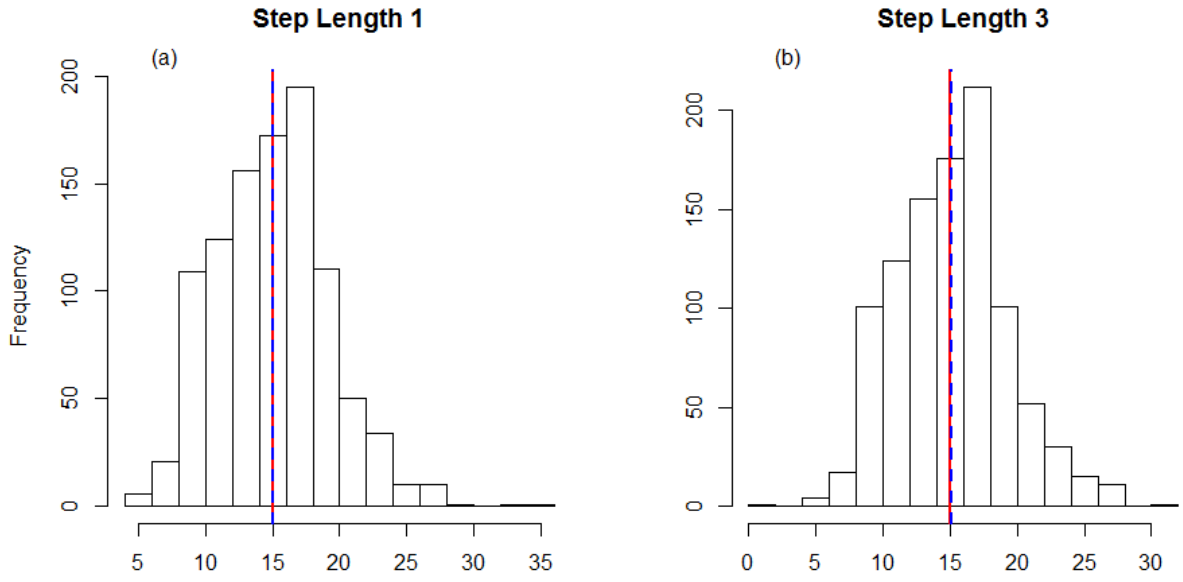

Figure 1-2. Histogram of abundance estimates from 1,000 simulated populations using the Instantaneous Sampling estimator. Animals in simulated populations took fixed steps with length 1 (a) or length 3 (b). The red line is truth (N = 15) and the blue line is mean estimated abundance.

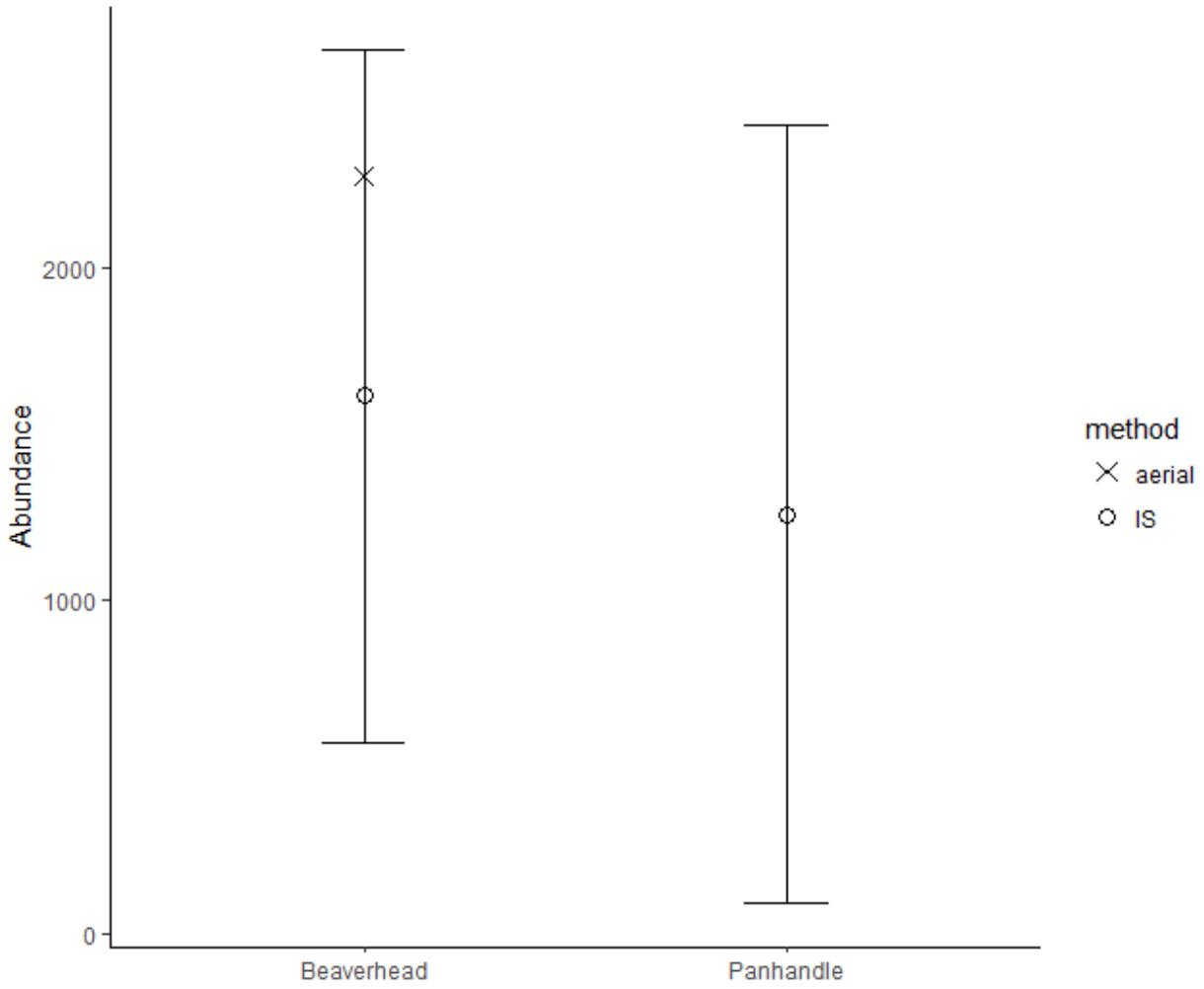

Figure 1-3. Instantaneous Sampling estimates of elk abundance (circles) for the Beaverhead and Panhandle study areas with 95% confidence intervals and the 2008 – 09 aerial survey estimate for the Beaverhead (cross). The IS method estimated 1,613 elk (SE 530) in the Beaverhead and 1,258 elk (SE 596) in the Panhandle for February 2016.

CHAPTER 2: TWO NEW MODELS TO ESTIMATE ABUNDANCE USING TIME-TO-EVENT ANALYSIS

ABSTRACT

Abundance is fundamental to ecology; accurate estimates are critical for understanding and managing populations. However, estimating abundance is frequently invasive, time-consuming, and expensive. Over the past few decades, remote traps such as cameras have been employed to estimate abundance noninvasively and less expensively. However, existing methods for estimating abundance from these data are quite limited when animals are not individually identifiable. In particular, these methods require arbitrary definitions of independent animal detections and knowledge of animals' home ranges and movement patterns, which are difficult to define. In order to address these challenges, we developed two new methods for estimating abundance of unmarked animals from remote trap data. We used time-to-event analysis as a new framework for estimating abundance from trapping rate. The resulting Space-to-Event (STE) and Time-to-Event (TTE) models use the Poisson-exponential relationship to estimate abundance from the first animal detection in a sample. We evaluated these models on simulated random walk data and applied them to a case study of remote camera data to estimate elk abundance. Simulation results suggested that the STE and TTE models were unbiased estimators of abundance. When applied to field data, these models produced abundance estimates that were comparable to those from a recent aerial survey. They also estimated elk abundance in an area where this has previously been impossible. This paper provides a new framework for estimating abundance of unmarked animals from remote trapping data that addresses many of the challenges from currently available methods.

INTRODUCTION

Understanding species' abundance is central to ecology (Andrewartha and Birch 1954). Ecologists use abundance to quantify population responses to changes in habitat, climate, or the presence of other species. Abundance can be a key factor in political and management decisions, including listing and delisting species under the Endangered Species Act (Doak et al. 2015) and setting sustainable harvest quotas (Williams et al. 2002). For centuries, scientists have estimated abundance from individuals with individually identifiable traits. LaPlace's ratio estimator (1786) eventually became the Lincoln-Petersen estimator (Petersen 1896, Lincoln 1930), and has since been expanded into dozens of capture-recapture models (Cooch and White 2017). However, many species have no natural markings that allow biologists to distinguish among individuals. Physically capturing animals to mark them is invasive, expensive, and frequently difficult to implement (Chandler and Royle 2013).

To estimate abundance from animals with no markings (natural or artificial, such as collars or tags), ecologists have developed a host of count methods. These include point counts, line transects, distance sampling, and N-mixture models (Williams et al. 2002, Royle 2004). For these methods, ecologists sample for short amounts of time to meet the assumption that animals are frozen in time and space. This assumption of closure on a small scale may be reasonably well met in certain systems like lakes, but violations can seriously bias abundance estimates (Williams et al. 2002).

Although movement is viewed as a nuisance for most count methods, it is actually useful information about the distribution of animals in space and thus, density (animals per unit area). In fact, spatial capture-recapture (SCR) models leverage animal movement to estimate abundance in a spatially defined area (Royle et al. 2014). Chandler and Royle (2013) extended

these SCR models to develop the Spatial Count (SC) model to estimate abundance of unmarked animals. However, the SC model assumes that there is a dense array of traps at different distances from each individual's home range center. Since the locations of home range centers are unknown beforehand, this is logistically quite difficult to implement. Furthermore, this assumption is untestable; there is no way to tell whether an unmarked individual visited multiple traps without an additional data source. Because of the difficulty of meeting these assumptions, few authors have applied this novel but challenging SC model.

Another new approach to estimating abundance from unmarked animals using movement is the Random Encounter Model (REM; Rowcliffe et al. 2008). To estimate abundance, the authors model contact rates between animals and remote camera traps. While this approach is promising, it requires independent estimates of animals' movement rates, which are challenging to obtain (Rowcliffe et al. 2008). Furthermore, this method requires that each detection of a species is independent of previous detections, so the authors implement a time cutoff between pictures to define independent encounters. While this approach is common, time cutoffs are arbitrary (e.g., 30 min, 1 hour, 1 day; Burton et al. 2015) and can be hard to define across different observed behaviors (e.g., transiting, bedding, foraging).

To address the challenges with currently available methods, we developed two novel methods to estimate abundance of unmarked animals using a continuous time-to-event framework. Time-to-event, or survival, models are used in fields as diverse as industry, medicine, and ecology, but have not yet been used to estimate abundance (Muenchow 1986). Ecologically, time-to-event models can estimate survival of animals (Cox and Oakes 1984), pollination rate (Muenchow 1986), and predator-prey encounters (Whittington et al. 2011). In recent statistical developments, they have been used to determine survey effort (Garrard et al.

2008) and estimate detection probability (Alldredge et al. 2007, Bischof et al. 2014). The time until detection of a species is related to abundance (McCarthy et al. 2013), but the exact relationship between the two has not yet been determined.

In this paper we develop two novel applications of the time-to-event framework to estimate animal abundance, based on the relationship between trapping rate and abundance. A trap can be any stationary device that records the presence or absence of animals over time, like camera traps (O'Connell et al. 2011) or acoustic recording devices (Dawson and Efford 2009). If traps are placed in areas of varying animal density, trapping rate increases as animal density increases (Carbone et al. 2001, Rowcliffe et al. 2008, Rovero and Marshall 2009). One interpretation of this relationship is spatial; if many traps record animal presence or absence at a single point in time, more traps should detect animals if abundance is high than if it is low. We used this relationship to develop the Space-to-Event (STE) model, which estimates abundance of unmarked animals from spatial trapping rate. This same framework also translates across time; at a single trap, the waiting time between animal detections should be shorter in areas of high abundance than low. Using this relationship, the Time-to-Event (TTE) model maximizes spatial and temporal information and can account for heterogeneous density. We evaluated these models with simulated random walk data then applied them to a case study of camera trap data to estimate elk (*Cervus elaphus*) abundance in Idaho, USA. The two models do not assume small-scale closure, they leverage animal movement during data collection, and they do not depend on arbitrary time cutoffs to define events.

METHODS

Space-to-Event Model

We developed a space-to-event (STE) model that uses spatial trapping rate to estimate abundance. Abundance is not directly observable, so we model it here as a latent variable. The Poisson distribution is frequently used to model abundance because it describes integer counts of animals that are randomly distributed in space (Royle 2004). To demonstrate this point, if a grid were overlaid on a landscape of randomly distributed animals, the number of animals N_i at a fixed point in time in any randomly selected grid cell i would be a random draw from the Poisson distribution. The parameter λ is the average number of animals in each grid cell, as shown in:

$$N_i \sim Pois(\lambda) \qquad \text{(Equation 1)}$$

To estimate λ, we analyzed spatial trapping rate data in a time-to-event framework. Time-to-event analyses describe the probability of some event of interest by observing the length of time before that event occurs (Cox and Oakes 1984). A special case of time-to-event analysis exists when the event of interest is Poisson distributed: the time until the first event is exponentially distributed (de Smith 2015). A classic example is cars passing through a stoplight. If cars move independently, the number of cars that pass through in a given amount of time is Poisson distributed and the time from any arbitrary starting point until the first car passes is exponentially distributed (Gerlough and Schuhl 1955).

This same relationship applies to space as well as time. For our purposes, the event of interest is a detection of one individual of the target species. The observed space-to-event is the number of random plots sampled before we find the species. We show here that when there are a Poisson number of animals in each grid cell, the space-to-event is exponentially distributed. If many grid cells can be sampled at a given moment in time j, as is possible when many traps are

deployed, the number of grid cells that must be sampled before the species is detected (S_i) is exponentially distributed, following:

$$S_j \sim Exp(\lambda) \quad \text{(Equation 2)}$$

To observe S_j, we sample random grid cells on a given instantaneous sampling occasion, j. We randomly draw one grid cell, and if it contains at least one animal, we record $S = 1$ and stop sampling. If it does not contain an animal, we draw another random grid cell. If this cell contains an animal, we record $S_j = 2$, and stop sampling. We continue these random draws until we find the first grid cell with an animal (Figure 2-1). We can repeat this process at multiple snapshots in time, $j = 1, 2, \ldots, J$ to create an encounter history of S_j. An example encounter history with $J = 5$ may look like $S_j = \{37, 5, NA, 1, 28\}$. This formulation assumes perfect detection within the grid cell, which we address later in this chapter.

In practice, we can only sample a finite number of grid cells on each sampling occasion. During some occasions, none of our sampled grid cells will contain animals. This is still informative; the space-to-event is longer than M, the number of sampled grid cells. This is a case of right-censoring, which is widely adopted in survival and time-to-event analyses (Muenchow 1986, Pyke and Thompson 1986, Castro-Santos and Haro 2003). In the encounter history above, we represent a right-censored sampling occasion as *NA*.

The STE model uses the observed encounter history to estimate λ from the exponential likelihood. We include right-censored data by integrating the upper tail of the exponential cumulative distribution function (CDF, indicated by $I_{(S \leq M)}$). The full likelihood for λ given the encounter history S_j over $j = 1, 2, \ldots, J$ sampling occasions in M sampled grid cells is

$$\mathcal{L}(\lambda | S_j) = \prod_{j=1}^{J} \left(I_{(S \leq M)} \lambda e^{-\lambda S_j} + I_{(1-(S \leq M))} \int_M^{\infty} 1 - e^{-\lambda S_j} \, d\lambda \right) \quad \text{(Equation 3)}$$

where the estimated $\hat{\lambda}$ is the average number of animals in each grid cell, or density per sampled unit. To estimate total abundance, we could draw an abundance $\hat{N_i}$, from the Poisson for each of the $i = 1, 2, \ldots, P$ grid cells in the study area and add them together. The sum of P independent Poisson random variables is a Poisson random variable with mean λP (Gallager 2013) so this is equivalent to $\widehat{N} \sim Pois(\hat{\lambda}P)$. Therefore, our estimate of $\hat{N}$ is based on the expected value of this distribution,

$$E[\widehat{N}] = \hat{\lambda}P \qquad \text{(Equation 4)}$$

The calculation of P is based on our sampling method. In practice, we randomly sample grid cells by deploying stationary traps, such as remote cameras. The trap itself defines the size and shape of the grid cells. This is a key point; the trap is not assumed to sample some larger area, the trap is in fact the grid cell. Trap areas may be irregularly shaped, but as long as the area is known, we can calculate P, the number of grid cells in the study area, with

$$P = \frac{A}{a} \qquad \text{(Equation 5)}$$

where A is the study area size and a is the trap area. The trap area a is equipment-specific. We demonstrate this method using remote cameras because they collect continuous data with time-stamped events, and we can calculate the visible area by published specifications. Although applied here to cameras, the general theory may apply to any kind of trap with a known area. For cameras, the trap area a is the circular sector defined by the lens angle θ (in degrees) and the trigger distance r

$$a = \pi r^2 \frac{\theta}{360} \qquad \text{(Equation 6)}$$

where θ/360 is the portion of a circle that is viewed by the camera.

We estimated the sampling variance of $\hat{N}$ using the properties of maximum likelihood theory and the Delta method (Cooch and White 2015). We constrained $\lambda \geq 0$ using the log-link

function $log(\lambda) = \beta$ before optimizing the likelihood. After optimizing, we estimated the sampling variance $\widehat{Var}(\hat{\beta}) = -[H]^{-1}$ where [*H*] was the estimated Hessian matrix. We then used the Delta method to estimate $\widehat{Var}(\hat{N})$ where $\hat{N} = P\hat{\lambda} = Pe^{\hat{\beta}}$. In the case of a single variable transformation such as $log(\lambda) = \beta$, the Delta method can be represented by

$$\widehat{Var}(\hat{N}) \approx \left(\frac{\partial N}{\partial \beta}\right)^2 \widehat{Var}(\hat{\beta}) \qquad \text{(Equation 7)}$$

where $\frac{\partial N}{\partial \beta} = Pe^{\beta}$ is the first order partial derivative of $\hat{N} = Pe^{\beta}$. This is an approximation of the sampling variance of $\hat{N}$.

Time-to-Event Model

We expanded the STE model into a Time-to-Event (TTE) model that can account for heterogeneous density across a landscape. The TTE model is based in the same theory as the STE model but uses observations in both time and space. Using the same Poisson-exponential relationship described above, the event of interest is still the first detection of the species of interest. However, instead of sampling at many traps at a single moment in time, here we sample a single trap for several consecutive periods in time. We record *T*, the first sampling period (*k*) in which we observe an animal (Figure 2-2). In practice, we sample grid cells by deploying traps such as cameras. As with the STE model, the trap itself defines the size and shape of the grid cell.

It is easiest to begin by thinking of each period *k* as a snapshot in time. In a given grid cell *i* at time *k* = 1, animals are either present or not. If they are present, the time-to-event is 1 (*T* = 1) and we stop sampling (assuming perfect detection for now). If animals are not present, we wait a short time to allow them to move, and we take another snapshot at time *k* = 2. We repeat this for several consecutive sampling *periods k* = 1, 2, …, *K* to complete a single sampling

occasion j. If we do not observe an animal during a given sampling occasion (i.e., on any of the *K* sampling periods), we right-censor this occasion (expressed here as *NA*). An example encounter history T_{ij} at trap $i = 1, 2, \ldots, M$ and occasion $j = 1, 2, \ldots, J$ with $K = 5$ sampling periods per sampling occasion is:

	Sampling occasion			
	1	2	3	4
Trap 1	3	1	NA	NA
Trap 2	NA	2	4	1
Trap 3	NA	NA	NA	5

We can estimate abundance when we make two constraints on the observation process. First, the length of time between each sampling period *k* should only be long enough to allow animals to move from one grid cell to a neighboring grid cell. Second, *k* should be small (e.g., five sampling periods per occasion). When these constraints are met, only animals from a localized cluster of grid cells are at risk of detection at a given trap and sampling occasion. Our observation of the first time-to-event is based on the average density in this cluster.

Within these constraints, the number of animals in a single grid cell *i* changes at each time *k*. In essence, this is the same as sampling several neighboring grid cells at a single instant in time. Instead, a single grid cell is sampled at consecutive points in time as the animals themselves move. This is essentially the STE model on a localized scale.

In practice, we let *k* be a period of time rather than a snapshot in time. The length of the period *k* follows the same constraint described above; it is equal to the amount of time it takes animals to move into a neighboring grid cell. This will depend on species' movement rates and the size of the grid cell. We used a rough approximation of this time unit and encourage future work to determine the exact relationship between movement rate, grid cell size, and time unit.

Once we have observed our encounter history T_{ij}, we estimate λ with the likelihood from the STE model, with an added dimension for the spatial replicates.

$$\mathcal{L}(\lambda|T_{ij}) = \prod_{j=1}^{J} \prod_{i=1}^{M} \left(I_{(T \leq K)} \lambda e^{-\lambda T_{ij}} + I_{(1-(T \leq K))} \int_{t}^{\infty} 1 - e^{-\lambda T_{ij}} \, d\lambda \right) \quad \text{(Equation 8)}$$

where $I_{(T \leq K)}$ indicates that an event occurred before the end of the given sampling occasion.

Because the TTE method uses replicates in both space and time, we can model heterogeneous density by adding a linear model to λ_i, the average density at grid cell *i* in the general form

$$\log(\lambda_i) = \beta_0 + \beta_1 x_{1i} + \beta_2 x_{2i} \quad \text{(Equation 9)}$$

where x_i are a site-specific covariates.

As with the STE model, we estimated abundance as $\hat{N} = \lambda P$. We calculated the variance of $\hat{N}$ using the estimated information matrix and the Delta method (Cooch and White 2015).

Simulation

We performed a mechanistic simulation to verify that the Space-to-Event and Time-to-Event models returned unbiased estimates of abundance. For each model, we simulated two populations of 15 animals moving at different speeds. Each "animal" was a list of xy-coordinates from an uncorrelated random walk of 1,000 steps, bounded within a 30x30 unit area. Each walk used fixed step lengths (length 1 for the "slow" population, and length 3 for the "fast" population) and random turning angles. For both models, we randomly placed 10 "traps," which were 1x1 unit squares. Animals were "captured" at a given trap and sampling occasion if their random walk coordinates fell within the trap's coordinates, inclusive of two borders. We ran 10,000 simulations for each population and model.

For the STE model, we sampled animals on every tenth step. We observed each trap in order and recorded the number of the first trap that captured an animal. This was our observation

of S_j at that sampling occasion. We repeated this on all sampling occasions, which created an encounter history of the first trap-to-event on 100 occasions.

For the TTE model, we sampled animals during 5-step sampling occasions (with each step as a sampling period). We started one sampling occasion every 15 steps. At each trap and sampling occasion, we recorded the number of steps until the first animal was caught in the trap. We repeated this at all traps and sampling occasions, which created an encounter history of first time-to-event on 67 occasions at 10 cameras.

Estimating elk abundance

Image classification

To evaluate the STE and TTE models on field data, we applied them to two sets of camera data to estimate elk abundance. For a detailed description of our study areas and field methods, refer to Chapter 1. In summary, we deployed 160 remote cameras in the Panhandle and Beaverhead study areas (defined by elk winter range) in February 2016. We randomly selected nine plots in each study area with Generalized Random Tessellation Sampling (GRTS, Stevens and Olsen 2004). We systematically placed nine cameras in each plot. In the Panhandle, we placed motion-triggered cameras on trees and cleared any vegetation obstructing their view. In the Beaverhead, we placed motion triggered and time lapse cameras on T-posts and placed flagging at known intervals in front of the camera. We only counted elk within a set distance of the camera to avoid miscounting and misclassification.

We calculated visible camera area in both study areas by camera specifications (TrailcamPro 2017). In the Beaverhead, we based visible camera area on the Reconyx HC600 model, letting $\theta = 42°$. We set $r = 50$m based on the flagging we deployed in the field. In the

Panhandle, we let $\theta = 45.2°$ and $r = 18.3$m, the maximum trigger distance (Reconyx model XR6).

Space-to-Event Model

For the STE model, we created temporally replicated encounter histories of the first camera until an elk detection. In each study area, we created a randomly ordered list of cameras. On each sampling occasion, we recorded S_j, the first camera on that list to detect an elk. Although the sampling should be instantaneous, we defined the sampling period as 1 minute to ensure we had enough detections. Any photos of elk during that one minute counted as a detection. We sampled each camera for one minute every 10 minutes, between 6-9 am and 6-9 pm from February 1-13, 2016. During the 583 sampling occasions, we recorded 208 observations in the Beaverhead and 33 observations in the Panhandle.

Time-to-Event Model

To implement the TTE model, we defined the sampling period length by estimating the average time for elk to move between grid cells. We defined the distance between grid cells as 30m, based on a 30x30m square, which was approximately the same area as a single Beaverhead camera. We calculated median elk speed from 122 GPS collars in the Beaverhead and Panhandle in January 2015, which was approximately 30 m/hr (IDFG unpublished data). From these calculations we set the sampling period length to one hour.

We created spatially and temporally replicated encounter histories of the time until first elk detection. We sampled every 8 hours throughout February 2016. Each four-hour sampling occasion consisted of four 1-hour periods. We recorded the first period in which an elk was detected, if any. If no elk were detected during a given sampling period, we right-censored that period.

RESULTS

Simulation

To evaluate the STE and TTE models, we estimated abundance from simulated data with a known population size. We applied the two models to two populations of 15 individuals moving at different speeds (slow and fast) to determine whether movement rate influenced estimated abundance.

The STE model appeared to produce an unbiased estimate of abundance for both populations (Figure 2-3). For the slow population, the mean estimated population size was 15.04 individuals. Mean estimated standard error through the Delta method was 3.78, whereas the standard error calculated from the 10,000 population estimates was 4.40. For the fast population, the mean estimated abundance was 14.97 individuals. Mean estimated standard error through the Delta method was 3.78. The standard error calculated from the repeated estimates was 4.10. This demonstrated that the model was not sensitive to movement rates of animals and that it performed as intended for randomly moving individuals.

The TTE model appeared to slightly underestimate abundance for both simulated populations (Figure 2-3). Coverage by the 95% confidence intervals was higher (86%) for the fast population than the slow population (64%). For the slow population, the mean estimated abundance was 12.52 individuals. The standard error calculated from the repeated estimates was 2.56 and the mean standard error estimated with the Delta method was 1.85. For the fast population, the mean estimated abundance was 14.30 and the mean estimated standard error from the Delta method was 1.98. The standard error calculated from the repeated estimates was 2.46.

Field

To evaluate the STE and TTE models in a real-world setting, we applied them to two sets of camera data to estimate elk abundance. We first checked the assumption that animals move independently. The elk in our camera traps mainly appeared in groups of one or two (Figure 2-4). Therefore, we believe this assumption was reasonably well met.

Over the 583 sampling occasions in the STE dataset, we recorded 208 observations in the Beaverhead and 33 observations in the Panhandle for the STE model. For the TTE model, over the 80 cameras and 84 sampling occasions, we recorded 101 elk detections in the Beaverhead and 80 detections in the Panhandle.

In the Beaverhead study area, the STE model estimated 1,405 elk (SE 133.4) and the TTE model estimated 2,217 elk (SE 211.6, Figure 2-5). The TTE estimate was comparable to the 2008-09 aerial survey estimates of 2,272 elk. In the Panhandle study area, the STE model estimated 1,368 elk (SE 238.4) and the TTE estimated 5,670 elk (SE 633.4). There were no existing estimates of elk abundance in this study area to compare with the STE and TTE estimates. Based on harvest statistics and expert knowledge of the area, these estimates appear to be within the range of possible values.

DISCUSSION

The two methods developed here represent a new framework for estimating abundance of unmarked animals. These novel applications of time-to-event analysis utilize continuous-time data in a new way. Simulation results suggested that the STE model was an unbiased estimator of abundance regardless of species' movement rate. The TTE simulation showed high coverage of the 95% confidence intervals for the simulated population moving at a faster speed. This indicated that the animals in the slower population had insufficient time to re-randomize at every

time step, which may have introduced correlation between the samples. The simulations also indicated that the Delta method underestimated the variance of $\hat{N}$. This was likely due to the non-linear transformation on λ and could be improved with a higher-order approximation (Cooch and White 2015).

Our camera trap case study demonstrated that the STE and TTE models could be used in the field to estimate abundance. In the Beaverhead study area, the TTE estimate was comparable to an independent estimate of abundance using an aerial survey. In both study areas, the STE estimate was lower than the TTE estimate, which may have been due to spatial autocorrelation among samples. Our nested study design likely led to high spatial correlation between cameras. This could have artificially inflated the observed space-to-event and deflated abundance estimates. Future implementations of the STE and TTE models should use random camera placement.

In the Panhandle study area, the STE and TTE methods allowed us to estimate elk abundance where no other methods to do so have been possible. The STE and TTE estimates differed from each other more in the Panhandle than in the Beaverhead. One potential explanation for this is that elk in the Panhandle were more restricted by steep slopes and dense vegetation than in the Beaverhead, which may have led to non-random movement among our cameras. Future efforts may explore the impact of violating the random movement assumption of our two models.

The time-to-event framework developed here helps address many challenges with estimating abundance from unmarked animals with remote trap data. First, N-mixture models and the Spatial Count (SC) model (Chandler and Royle 2013) are sensitive to trap spacing. It can be difficult to determine animal home range size and movement patterns ahead of time, which

can bias estimates if not done correctly (Chandler and Royle 2013, Keever 2014). Because the STE and TTE models are based in random sampling of the landscape rather than within the (unknown) home range of an individual, they are not sensitive to trap spacing. Second, the Random Encounter Model (REM) (Rowcliffe et al. 2008) requires classification of independent contacts between animals and the cameras. Across a string of photos, biologists must make arbitrary definitions of independent contacts, often using time cutoffs or other criteria (Burton et al. 2015). Because the STE and TTE methods use randomized sampling, they do not require this kind of definition of independent contacts. Finally, the Random Encounter Model (REM) requires independent estimates of species' movement rates, which can be difficult to obtain (Rowcliffe et al. 2014). The STE uses snapshots in time, so estimates are independent of movement rate. The TTE model reduces the impact of movement rate by using short sampling occasions.

When applied to camera trap data, the STE and TTE methods improve upon several camera-specific issues. First, they eliminate the need to count group size from a series of photos. The SC model and N-mixture models require accurate counts of individuals at each trap, which can be prohibitive for some species. For instance, elk tend to mill around cameras, moving in and out of view over a long period of time, which makes counting individuals impossible. In contrast, the STE and TTE models depend solely on the first detection of an animal, so there is no need to count individuals. The STE and TTE models also greatly decrease the number of photos required for analysis. Currently, tens of thousands of remote cameras are deployed around the world, which produce millions of pictures (Steenweg et al. 2017). Until photograph classification can be fully automated, large-scale camera trap studies are limited by the man hours required to classify

millions of pictures. By using only the first animal detection on each occasion, The STE and TTE models use only a sample of photos, which can greatly decrease this workload.

As with any observation method, detection of animals is rarely perfect in the field. Abundance estimates can be biased low unless imperfect detection is taken into account (MacKenzie et al. 2002). We suggest a future extension of the STE and TTE models to account for imperfect detection that uses the geometric and gamma distributions. It is described here in the context of the TTE model. A trap with imperfect detection may miss an animal on its first z visits to a trap, but capture it on the (z+1)st visit. The sum of exponential waiting times is gamma distributed, so the waiting time until the (z+1)st visit is a gamma distributed random variable (Mood et al. 1974). The full likelihood of λ_i uses observations of T_{ij}, the gamma distributed time-to-event at trap $i = 1, 2, \ldots, M$ on occasion $j = 1, 2, \ldots, J$ with $k = 1, 2, \ldots, K$ sampling periods per occasion. It also uses z, a geometric-distributed count of the number of occasions missed. Right-censored occasions are indicated by $I_{(1-(T\leq K))}$ when there are no observations by the end of the sampling occasion j. The full likelihood in the shape-rate formulation is

$$\mathcal{L}(\lambda_i|T_{ij}) = \prod_{j=1}^{J}\prod_{i=1}^{M}\sum_{z=0}^{\infty}\left(I_{(T\leq K)}p(1-p)^z\frac{\lambda_i^{z+1}}{\Gamma(z+1)}T_{ij}^z e^{-\lambda_i T_{ij}} + I_{(1-(T\leq K))}p(1-p)^z\int_t^{\infty}\frac{1}{\Gamma(z+1)}\gamma(z+1,\lambda_i T_{ij})d\lambda\right) \quad \text{(Equation 10)}$$

Further development of the geometric-gamma formulation is needed because there is a near singularity in the Hessian matrix.

The STE and TTE models developed here are a novel approach for estimating abundance of unmarked animals. Previous methods for estimating abundance from unmarked animals ignore the relationship between animal encounter rate and abundance, which our models exploit. Additional work on the TTE model may adjust the estimation of the length of the sampling period k to more accurately reflect the relationship between movement and trap size. The STE

and TTE models fit naturally with camera data, and we encourage future work into applications with other continuous-time data. The time-to-event framework developed in this paper is a promising path forward toward completely non-invasive population monitoring.

LITERATURE CITED

Alldredge, M. W., K. H. Pollock, T. R. Simons, J. A. Collazo, and S. A. Shriner. 2007. Time-of-detection method for estimating abundance from point-count surveys. The Auk 124:653–664.

Andrewartha, H. G., and C. Birch. 1954. The distribution and abundance of animals. First edition. University of Chicago Press, Chicago.

Bischof, R., S. Hameed, H. Ali, M. Kabir, M. Younas, K. A. Shah, J. U. Din, and M. A. Nawaz. 2014. Using time-to-event analysis to complement hierarchical methods when assessing determinants of photographic detectability during camera trapping. Methods in Ecology and Evolution 5:44–53.

Burton, A. C., E. Neilson, D. Moreira, A. Ladle, R. Steenweg, J. T. Fisher, E. Bayne, and S. Boutin. 2015. Wildlife camera trapping: a review and recommendations for linking surveys to ecological processes. Journal of Applied Ecology 52:675–685.

Carbone, C., S. Christie, K. Conforti, T. Coulson, N. Franklin, J. R. Ginsberg, M. Griffiths, J. Holden, K. Kawanishi, M. Kinnaird, R. Laidlaw, A. Lynam, D. W. MacDonald, D. Martyr, C. McDougal, L. Nath, T. O'Brien, J. Seidensticker, D. J. L. Smith, M. Sunquist, R. Tilson, and W. N. Wan Shahruddin. 2001. The use of photographic rates to estimate densities of tigers and other cryptic mammals. Animal Conservation 4:75–79.

Castro-Santos, T., and A. Haro. 2003. Quantifying migratory delay: a new application of survival analysis methods. Canadian Journal of Fisheries and Aquatic Sciences 60:986–996.

Chandler, R. B., and J. A. Royle. 2013. Spatially explicit models for inference about density in unmarked or partially marked populations. Annals of Applied Statistics 7:936–954.

Cooch, E. G., and G. C. White, editors. 2017. Program MARK: A Gentle Introduction. 17th edition.

Cooch, E., and G. C. White. 2015. Appendix B - The "Delta method"... Program MARK: A gentle introduction 1:1–29.

Cox, D. R., and D. Oakes. 1984. Analysis of survival data. First edition. CRC Press.

Dawson, D. K., and M. G. Efford. 2009. Bird population density estimated from acoustic signals. Journal of Applied Ecology 46:1201–1209.

Doak, D. F., G. K. H. Boor, V. J. Bakker, W. F. Morris, A. Louthan, S. A. Morrison, A. Stanley, and L. B. Crowder. 2015. Recommendations for improving recovery criteria under the US Endangered Species Act. BioScience 65:189–199.

Gallager, R. G. 2013. Poisson processes. Pages 74–108Stochastic Processes: Theory for Applications. Cambridge University Press, New York.

Garrard, G. E., S. A. Bekessy, M. A. McCarthy, and B. A. Wintle. 2008. When have we looked hard enough? A novel method for setting minimum survey effort protocols for flora surveys. Austral Ecology 33:986–998.

Gerlough, D. L., and A. Schuhl. 1955. Use of Poisson distribution in highway traffic. Eno Foundation for Highway Traffic Control.

Keever, A. C. 2014. Use of N-mixture models for estimating white-tailed deer populations and impacts of predator removal and interspecific competition.

LaPlace, P. S. 1786. Sur les naissances, les mariages et les morts. Page 693–702. Histoire de L'Academie Royale des Sciences. Paris.

Lincoln, F. C. 1930. Calculating waterfowl abundance on the basis of banding returns.

MacKenzie, D. I., J. D. Nichols, G. B. Lachman, S. Droege, J. Andrew, and C. A. Langtimm. 2002. Estimating site occupancy rates when detection probabilities are less than one. Ecology 83:2248–2255.

McCarthy, M. A., J. L. Moore, W. K. Morris, K. M. Parris, G. E. Garrard, P. A. Vesk, L. Rumpff, K. M. Giljohann, J. S. Camac, S. S. Bau, T. Friend, B. Harrison, and B. Yue. 2013. The influence of abundance on detectability. Oikos 122:717–726.

Mood, A. M., F. A. Graybill, and D. C. Boes. 1974. Introduction to the Theory of Statistics. Third edition. McGraw-Hill, Singapore.

Muenchow, G. 1986. Ecological use of failure time analysis. Ecology 67:246–250.

O'Connell, A. F., J. D. Nichols, and K. U. Karanth, editors. 2011. Camera traps in animal ecology: methods and analyses.

Petersen, C. G. J. 1896. The yearly immigration of young plaice into the Limfjord from the German Sea. Report of the Danish Biological Station 6:1–48.

Pyke, D. A., and J. N. Thompson. 1986. Statistical analysis of survival and removal rate experiments. Ecology 67:240–245.

Rovero, F., and A. R. Marshall. 2009. Camera trapping photographic rate as an index of density in forest ungulates. Journal of Applied Ecology 46:1011–1017.

Rowcliffe, J. M., J. Field, S. T. Turvey, and C. Carbone. 2008. Estimating animal density using camera traps without the need for individual recognition. Journal of Applied Ecology 45:1228–1236.

Rowcliffe, J. M., R. Kays, B. Kranstauber, C. Carbone, and P. A. Jansen. 2014. Quantifying levels of animal activity using camera-trap data. Methods in Ecology and Evolution

5:1170–1179.

Royle, J. A. 2004. N-Mixture Models for Estimating Population Size from Spatially Replicated Counts. Biometrics 60:108–115.

Royle, J. A., R. B. Chandler, R. Sollmann, and B. Gardner. 2014. Spatial capture-recapture. Elsevier.

de Smith, M. J. 2015. STATSREF: Statistical Analysis Handbook - a web-based statistics resource. The Winchelsea Press, Winchelsea, UK.

Steenweg, R., M. Hebblewhite, R. Kays, J. Ahumada, J. T. Fisher, C. Burton, S. E. Townsend, C. Carbone, J. M. Rowcliffe, J. Whittington, J. Brodie, J. A. Royle, A. Switalski, A. P. Clevenger, N. Heim, and L. N. Rich. 2017. Scaling up camera traps: monitoring the planet's biodiversity with networks of remote sensors. Frontiers in Ecology and the Environment 15:26–34.

Stevens, D. L., and A. R. Olsen. 2004. Spatially balanced sampling of natural resources. Journal of the American Statistical Association 99:262–278.

TrailcamPro. 2017. Reconyx game camera reviews. https://www.trailcampro.com.

Whittington, J., M. Hebblewhite, N. J. Decesare, L. Neufeld, M. Bradley, J. Wilmshurst, and M. Musiani. 2011. Caribou encounters with wolves increase near roads and trails: A time-to-event approach. Journal of Applied Ecology 48:1535–1542.

Williams, B. K., J. D. Nichols, and M. J. Conroy. 2002. Analysis and management of animal populations. Academic Press.

FIGURES

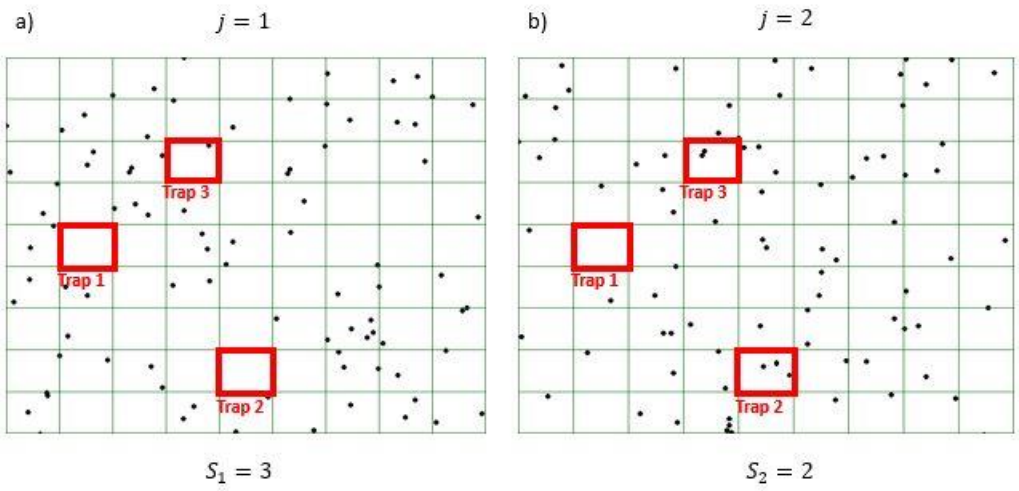

Figure 2-1. Conceptual diagram of the Space-to-Event (STE) model. An array of grid cells with known area are randomly sampled. In the case of cameras, the shape of the grid cell is a circular sector rather than a rectangle. On each occasion $j = 1, 2, \ldots, J$ the observed space-to-event S_j is the number of the first trap $i = 1, 2, \ldots, M$ (here, $M = 3$) that contains the species of interest. a) At $j = 1$, the first trap that contains an animal is trap 3, so $S_1 = 3$. b) At $j = 2$, although both traps 2 and 3 contain an animal, we record the first trap in the series {2, 3}, so $S_2 = 2$.

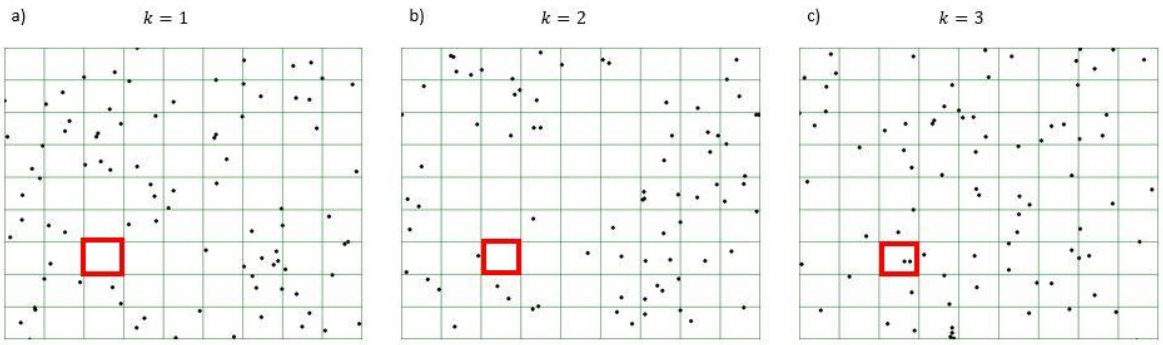

Figure 2-2. Conceptual diagram of the Time-to-Event (TTE) model at a single trap *i* and a single occasion *j*. When using cameras, the shape of the grid cell is a circular sector rather than a rectangle. Successive samples are taken at each period $k = 1, 2, \ldots, K$ (Here, $K = 3$). The observed time-to-event T_{ij} is equal to the period k in which the grid cell first contains an animal. There are no animals in the trap in a) $k = 1$ or b) $k = 2$, so for this camera and sampling occasion, $T_{ij} = 3$.

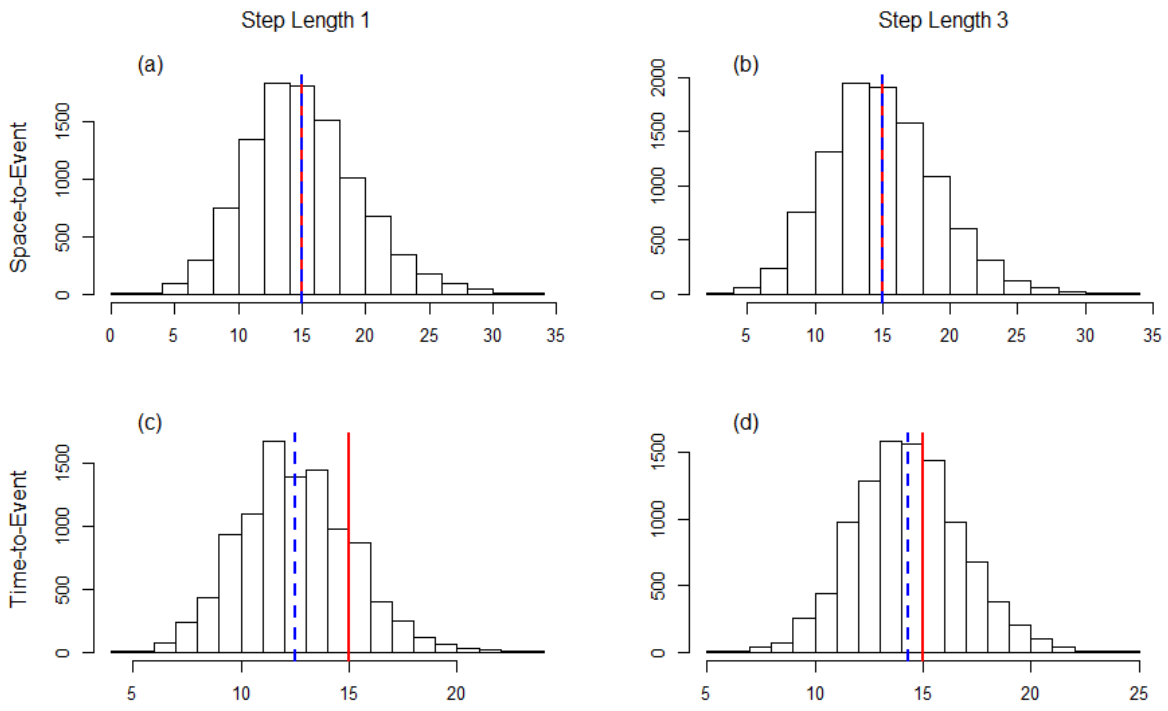

Figure 2-3. Histogram of abundance estimates from 10,000 simulated populations using the Space-to-event (a, b) and Time-to-Event (c, d) models. Simulated animals took fixed steps with either length 1 (a, c) or length 3 (b, d). The red line is truth (N = 15) and the blue line is mean estimated abundance.

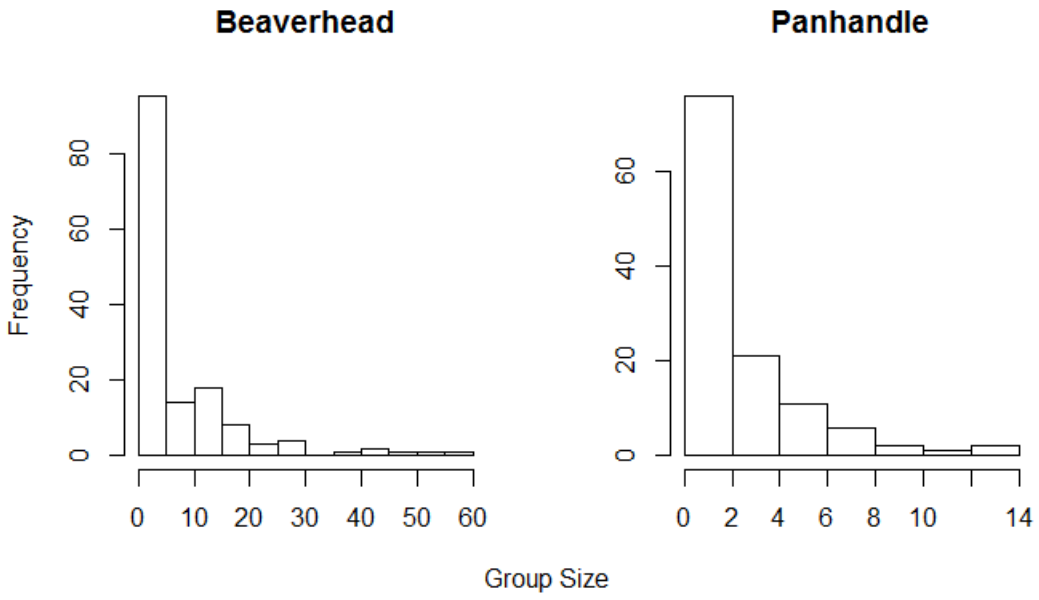

Figure 2-4. Elk group size from the Beaverhead and Panhandle camera data in February 2016. Most elk occurred in groups of 1 or 2.

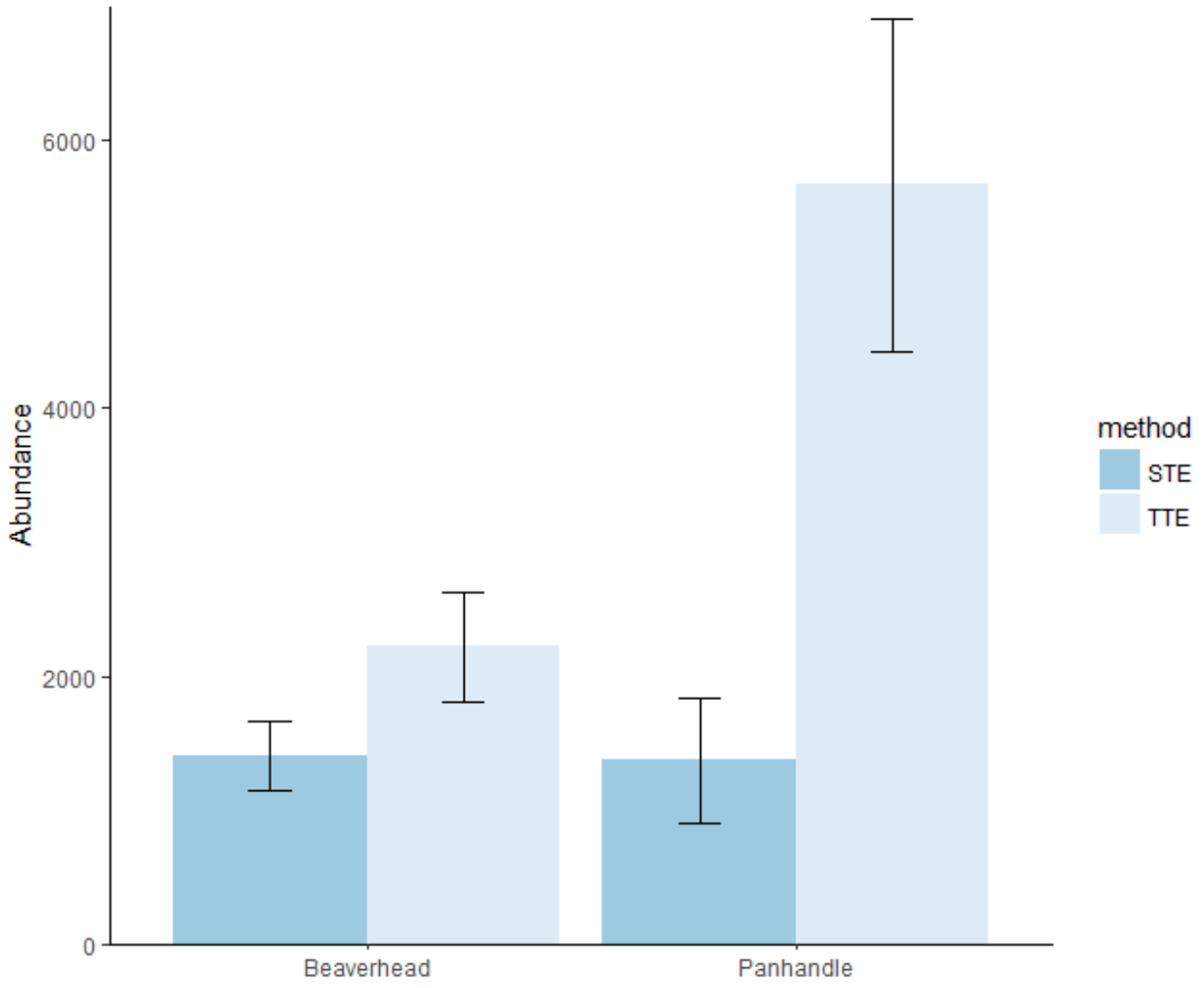

Figure 2-5. Space-to-Event (STE) and Time-to-Event (TTE) estimates of elk abundance in the Beaverhead and Panhandle study areas with 95% confidence intervals. In the Beaverhead study area, the STE model estimated 1,405 elk (SE 133.4) and the TTE model estimated 2,217 elk (SE 211.6). In the Panhandle study area, the STE model estimated 1,368 elk (SE 238.4) and the TTE estimated 5,670 elk (SE 633.4).